A novel diode laser system for photodynamic therapy

Samsöe Andersen, Eva; Petersen, PM; Andersen, PE; Andersson-Engels, Stefan; Svanberg, Katarina

Published in:
LASER-TISSUE INTERACTIONS, THERAPEUTIC APPLICATIONS, AND PHOTODYNAMIC THERAPY

DOI:
10.1117/12.446515

2001

A novel diode laser system for photodynamic therapy

Eva Samsøe* [a, b], Paul M. Petersen[a], Peter E. Andersen[a],
Stefan Andersson-Engels[b] and Katarina Svanberg[b]

[a]Risø National Laboratory, P.O Box 49, DK-4000 Roskilde, Denmark
[b]Lund Institute of Technology, Lund University, Box 118, SE-221 00 Lund, Sweden

ABSTRACT

In this paper a novel diode laser system for photodynamic therapy is demonstrated. The system is based on linear spatial filtering and optical phase conjugate feedback from a photorefractive $BaTiO_3$ crystal. The spatial coherence properties of the diode laser are significantly improved. The system provides an almost diffraction limited output which is efficiently coupled into a 50 μm core diameter fiber. The optical power transmitted through the fiber is increased by a factor of six when the feedback is applied to the diode laser. 85 percent of the power from the freely running laser diode is extracted in a high-quality beam and 80 percent of the output power is extracted through the fiber. The power transmitted through the fiber scales linearly with the power of the laser diode, which means that a laser diode emitting 1.7 W multi-mode radiation would provide 1 W of optical power through a 50 μm core diameter fiber. The system is compact, portable, stable, and easy to operate.

Keywords: Photodynamic therapy, Diode lasers, Medical optics instruments

1. INTRODUCTION

Photodynamic therapy (PDT) is a promising treatment modality of malignant and pre-malignant tumors.[1–4] PDT relies on the coexistence of three components: photosensitizer, light, and oxygen. The photosensitizer is administered to the patient, where it accumulates selectively in the cancerous cells. When the light excites the photosensitive drug a photochemical reaction occurs. This leads to the formation of singlet oxygen, which is a reactive and highly aggressive molecule. The singlet oxygen reacts with its surroundings, i.e. the diseased tissue, causing selective destruction of the cancerous cells. Using the photosensitizer δ-aminolevulinic acid (δ-ALA) requires light with a wavelength around 635 nm.

The use of diode laser systems in medicine has increased rapidly during the past decade since their compactness, low cost, and simple operation make them attractive in a clinical environment. They are continuously replacing light sources previously used in PDT - large expensive systems that, in addition, are complex to operate.[5] A remaining drawback of presently available diode laser systems is that they provide a low-quality laser beam. This means that they have poor coupling efficiency to small-core diameter optical fibers and are only capable of delivering the treatment light through optical fibers with core diameters of 400 μm or more. This limitation is especially important to PDT. For this application it can be difficult to find a laser with sufficient power through a thin fiber for optimal treatment. The optimal fiber size in individual treatment cases is often less than 400 μm. When performing interstitial PDT treatments, it is desirable to have a thin treatment fiber. Thus, there is a need for a new light source delivering the therapeutic light through an optical fiber with a small core diameter.

Frequency selective (FS) phase conjugate feedback (PCF) has proven an efficient method for enhancement of the output from laser diodes.[6,7] In this scheme a broad area laser (BAL) or a laser diode array (LDA) is exposed to external phase conjugate feedback[8,9] from a self-pumped, photorefractive crystal.[10,11] Furthermore, the system includes a spatial filter and a frequency selective element (e.g. a Fabry-Perot etalon). The scheme forces the laser diode to operate with high temporal coherence and to exhibit an almost diffraction limited output.

In this work, we investigate the spatial improvement and the temporal stability of a broad area laser implemented in a similar scheme. We observe a highly improved output from a 637 nm BAL. The quality of the beam is evaluated by measuring the M^2 beam quality factor, which is a measure of how well the beam can be focused.[12] Approximately 85 percent of the multi-mode power from the freely running BAL is extracted in an almost diffraction limited output.

* Contact E. Samsøe: e-mail: eva.samsoe@risoe.dk, Optics and Fluid Dynamics Department, Risø National Laboratory, phone: (+45) 4677 4553.

Laser-Tissue Interactions, Therapeutic Applications, and Photodynamic Therapy,
Reginald Birngruber, Hubert van den Bergh, Editors, Proceedings of SPIE Vol. 4433
(2001) © 2001 SPIE · 1605-7422/01/$15.00

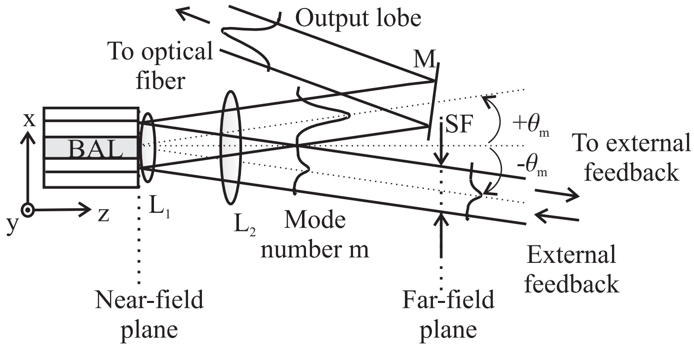

Figure 1. Side view of the feedback scheme in use. The low intensity lobe is directed to the phase conjugator, while the high intensity lobe constitutes the output from the system that is coupled into the 50 μm fiber. BAL is the broad area laser, L_1 and L_2 are collimating lenses, SF is the spatial filter, and M is a mirror. $\pm\theta_m$ denotes the angles between the center of radiation from the BAL and the peak intensities of the lobes in mode m.

Approximately 80 percent of the output power from the laser system is coupled through a 50 μm core-diameter fiber. The system was used in a clinic, where preliminary clinical trials were performed on two Wistar/Furth rats with colon adenocarcinoma inoculated into the muscles of the hind legs.

2. EXPERIMENTS

The setup scheme can be explained from Fig. 1 as follows. The output from a multi-mode diode laser consists of a superposition of lateral broad area modes.[13] Each of the modes constitutes a double lobed intensity profile in the far field. The different modes are distinguished by different frequencies and radiation angles. Mode number m exhibits two symmetrical lobes in the far-field plane, with peak intensities radiated at angles $\pm\theta_m$, with respect to the normal of the emitting aperture of the laser, i.e. the z-axis. The fundamental mode is radiated at the angle $\theta = 0$. By the insertion of a spatial filter one can choose a single lobe of the double lobed profile to pass. The linear spatial filter is placed in the far-field plane defined by the collimating lenses L_1 and L_2. The lobe transmitted through the spatial filter is retro-reflected by the phase conjugator and re-injected into the laser medium. This causes the laser to prefer lasing in one spatial mode. The resulting single-mode radiation is strongly asymmetric with a dominant lobe, referred to as the output lobe, and a smaller lobe, referred to as the injection lobe. As shown in Fig. 1 the smaller lobe runs between the diode laser and the external reflector, locking the diode laser in a single spatial mode operation.

The experimental setup shown in Fig. 2 illustrates a GaAlAs broad area single-stripe laser (HPD1302-TO3-TEC) implemented in the feedback system. The external reflector is a photorefractive $BaTiO_3$ crystal acting as a phase conjugate mirror (PCM). The crystal is arranged in the self-pumped Cat geometry, which is based on internal reflections inside the crystal.[14] The dimensions of the emitting aperture of the BAL are 1 μm in the transverse (the high coherence axis - y) and 100 μm in the lateral (the low coherence axis - x) direction. The laser is linearly polarized in the y-direction, which is also the high coherence axis of the laser. The maximum output power of the freely running laser is 200 mW. This power is obtained at a drive current of 550 mA $\simeq 1.7 \times I_{th}$, where I_{th} denotes the threshold current of the BAL, $I_{th} = 330$ mA for the freely running laser. The bandwidth (FWHM) of the BAL is 0.7 nm. L_1 and L_2 constitute a collimating lens pair with focal lengths of 4.5 mm (aspherical) and 40 mm (cylindrical) respectively, while W is a wedge extracting two reflections to beam diagnostics. E is an optional frequency selective element (e.g. a Fabry-Perot etalon) that, when inserted correctly, forces the BAL to oscillate in a single frequency.[7] The etalon may be omitted, since the absorption band of the photosensitizer is relatively large as compared with the bandwidth of the laser.[4] SF denotes the spatial filter and is placed in the far-field plane defined by L_1 and L_2. The lens L_3 slightly focuses the beam onto the PCM at an angle of approximately 50°. The $BaTiO_3$ crystal measures $5.41 \times 5.35 \times 6.98$ mm^3 (a × a × c). It is oriented so that the high coherence axis (y), the polarization of the BAL, and the crystal c-axis lie in the same plane, which yields the highest photorefractive response.[15] The scheme forces

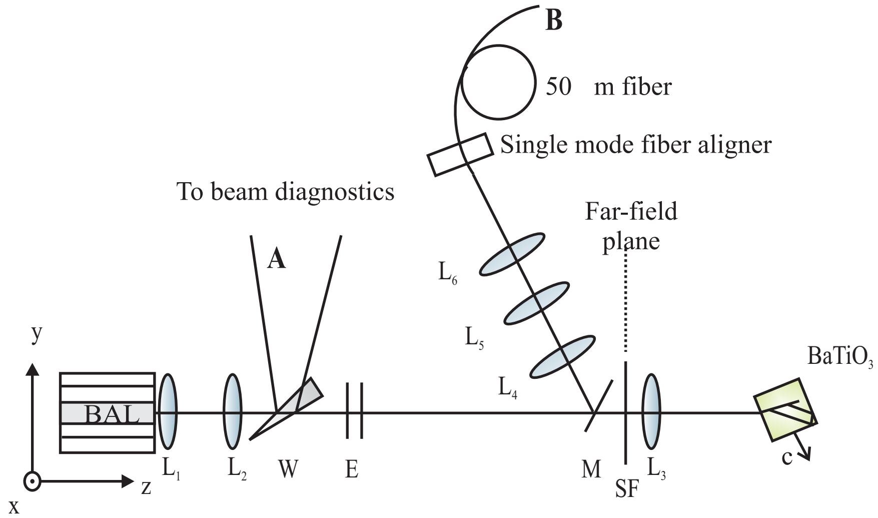

Figure 2. Top view of the experimental setup for single-mode fiber coupled BAL. L_1 and L_2 are collimating lenses, W is a wedge extracting two reflections for beam diagnostics, E is an optional etalon, SF is a spatial filter, L_3 is a focusing lens, M is the output coupler, L_4 and L_5 expand the beam in the lateral direction, and L_6 is an achromat coupling the beam into the fiber. The coordinate system represents the lateral (x), the transverse (y), and the longitudinal (z) axes respectively. **A** and **B** denote particular measurement positions referred to in the text.

the laser to emit single-mode radiation where one of the lobes (the output lobe) is amplified. The high-power lobe is extracted from the system by the mirror M, as shown in Fig. 1.

The output is collimated in the high coherence axis, but is slightly diverging in the low coherence axis. In order to couple the output into an optical fiber with a core diameter of 50 μm, the beam is expanded in the lateral direction to obtain an approximately circular shape before the beam is focused into the fiber. The beam expanding system consists of two cylindrical lenses of focal lengths 5 mm (L_4) and 40 mm (L_5), respectively. The beam is coupled into the optical fiber using an achromat (L_6) with a focal length of 40 mm.

The length of the setup is 30 cm and it was built on a lightweight honeycomb breadboard of dimensions 45 × 60 cm^2 for portability.

3. RESULTS

3.1. Spatial Characteristics

The lateral far-field pattern, i.e. the intensity distribution, was measured as a function of radiation angle. The distributions were measured in the beam path marked **A** in Fig. 2. They were measured in the far-field plane defined by L_1 and L_2. Figure 3 shows the results at three different drive currents: a) 1.3 × I_{th}, b) 1.4 × I_{th}, and c) 1.7 × I_{th}, respectively. The full-line curves indicate the distribution when the PCM and spatial filtering are applied, while the dashed curves show the behavior of the freely running laser. As can be observed from the figure, the double lobe profile is maintained even at high drive currents. The beam quality factor M^2 is enhanced from an $M^2 = 8$ when the laser is freely running to $M^2 = 1.6$ when the feedback scheme is applied at a drive current of 1.3 × I_{th}. At I=1.7 × I_{th} the M^2 is improved from 9 to 1.9.

3.2. Fiber Coupling

The fiber is a 50 μm core diameter glass fiber with a numerical aperture of 0.25. Figure 4 shows the optical power from the fiber as a function of drive current when the feedback scheme is applied (dots) and when the laser runs freely (cross hairs), respectively. The measurements are performed at the position marked **B** in Fig. 2. As can be seen from the figure, a considerably larger amount of light is coupled through the fiber when the phase conjugate feedback and the spatial filtering are included. At I = 1.3 × I_{th} = 430 mA the system increases the output power

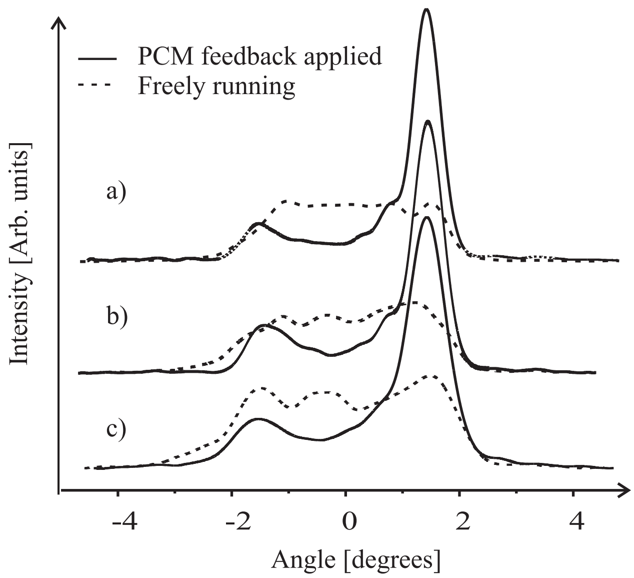

Figure 3. Intensity distributions in the far field with and without PCM feedback in the far field. The intensities are shown in arbitrary units as a function of lateral radiation angle. Distributions are shown for drive currents: a)1.3 × I_{th}, b)1.4 × I_{th}, and c)1.7 × I_{th}. Note that the double lobe profile is maintained even at the highest drive current.

from the fiber by a factor of 15. This means that the laser system is highly efficient as compared with the freely running laser. 80 percent of the output power from the laser system was coupled through the fiber.

3.3. Output Stability

The long-term stability of the power from the system was examined in a 20 hours "hands-off" measurement. The power was measured every 60 seconds and the results are shown in figs. 5 (a)-(b). Figure 5 (a) demonstrates the output power from the 50 μm fiber when the feedback system is applied, i.e. the data are measured at position **B** in Fig. 2. For comparison, figure 5 (b) shows the stability of the freely running laser in a similar experiment and at the same drive current (1.3 × I_{th}). These data are measured just in front of the BAL. The standard deviations are 3.3 and 3.6 percent in (a) and (b), respectively. The figure indicates that the system with PCF (a) is globally more stable than without feedback (b). The local noise, however, is somewhat larger in the external feedback system than for the freely running laser. The difference in the noise levels may be attributed to a longitudinal mode competition phenomenon. In the case of the freely running diode laser, a number of longitudinal modes oscillate simultaneously.[16] Only the total intensity, not the single mode, of the laser is stabilized. This leads to a strong cancellation between the anti-correlated fluctuations of the main mode and the additional weak modes, resulting in a low overall noise amplitude. In the PCF system, on the other hand, fewer longitudinal modes oscillate and the spectrum is narrowed down due to the PCF.[7] In this case the mode cancellation is not as pronounced and a larger noise level is observed. Moreover, the feedback from the PCM may generate external cavity modes that also contribute to the noise. The PCF indeed leads to an increase in intensity noise and several characteristic external cavity-resonance peaks are identified in the spectrum.[17]

3.4. Clinical Trials

Preliminary clinical animal trials were performed at Lund University Hospital in Sweden. ALA-PDT was performed on two Wistar/Furth rats, each weighting approximatly 250 g, with colon adenocarcinoma inoculated into the muscle of the hind leg. These results, however, have not been completed yet.

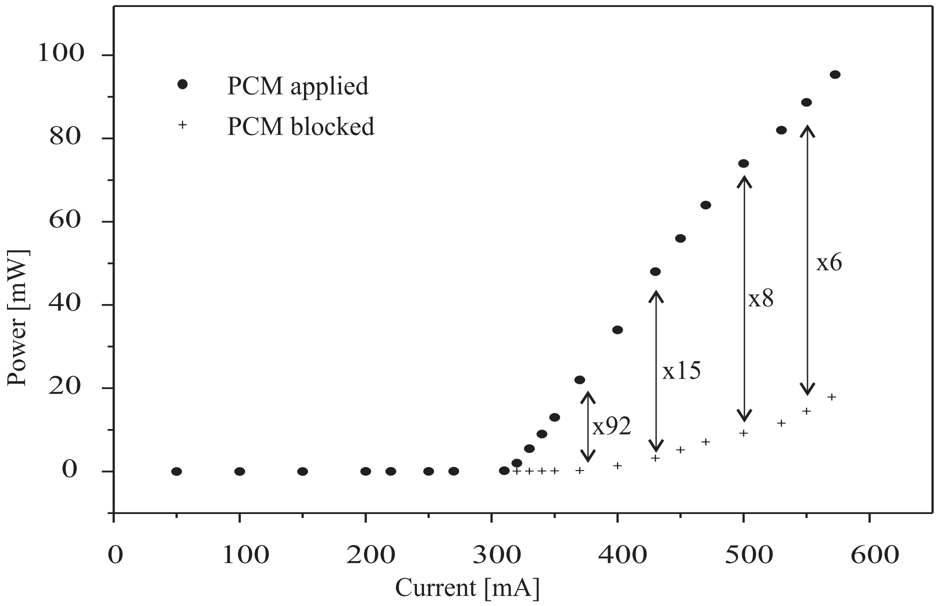

Figure 4. Power-current characteristics from the 50 μm core diameter fiber when the feedback system is applied (dots) vs. when the laser runs freely (cross hairs). The feedback system ensures a large conversion of multi-mode radiation into a high-quality almost diffraction limited beam that couples well to the fiber.

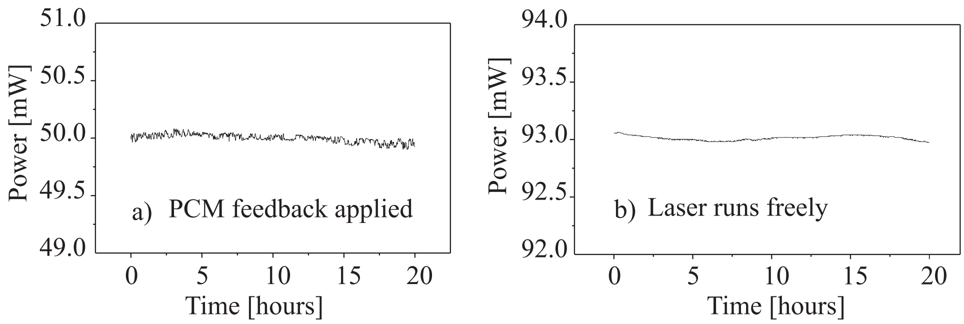

Figure 5. Power stability measurements during 20 hours of "hands-off" operation of (a) the output from the fiber and (b) the freely running laser. The standard deviations are (a) 3.3 percent and (b) 3.6 percent, respectively. Both measurements are performed at I = 1.3 × I_{th}.

4. DISCUSSION AND CONCLUSION

We have demonstrated a novel diode laser system for PDT. The system drastically improves the spatial characteristics of the diode laser and the output is efficiently coupled into an optical fiber with small core diameter.

At 1.3 times the threshold current (430 mA), the M^2 of the BAL was decreased from 8 to 1.6 due to the spatial filtering and the PCM feedback. 85 percent of the multi-mode radiation was extracted in an almost diffraction limited output. The power obtained from the 50 μm fiber was increased by a factor of six compared with the output from the fiber when the laser was running freely. The maximum output power from the system delivered through the fiber was approximately 110 mW, corresponding to 80 percent of the maximum output from the system.

Since the power transmitted through the fiber scales linearly with the power of the laser diode, this facilitates the design of an efficient and compact diode laser system for (interstitial) PDT. The maximum output from the fiber can be increased by incorporating a BAL or LDA with higher power in the scheme. With the conversion efficiency found in this study, a BAL/LDA emitting around 1.7 W multi-mode radiation would provide approximately 1 W through the 50 μm fiber.

ACKNOWLEDGMENT

This work was supported by the Danish Technical Research Council grant number 9901433.

REFERENCES

1. T. J. Dougherty, "Photoradiation therapy for cutaneous and subscutaneous malignancies," *J. Invest. Dermatol.* **77**, p. 122, 1981.
2. D. Ash and S. B. Brown, "Photodynamic therapy - achievement and prospects," *Br. J. Cancer* **60**, p. 151, 1989.
3. I. Wang, N. Bendsøe, C. af Klinteberg, A. M. K. Enejder, S. Andersson-Engels, S. Svanberg, and K. Svanberg, "Photodynamic therapy vs. cryosurgery of basal cell carcinomas: results of a phase III clinical trial," *Br. J. Dermatol.* **144**, p. 832, 2001.
4. Q. Peng, T. Warloe, K. Berg, J. Moan, M. Kongshaug, K.-E. Giercksky, and J. M. Nesland, "5-aminolevulinic acid-based photodynamic therapy: clinical research and future challenges," *Cancer* **79**, p. 2282, 1997.
5. I. Wang, *Photodynamic Therapy and Laser-Based Diagnostic Studies of Malignant Tumours.* PhD thesis, Lund University, 1999.
6. S. MacCormack and J. Feinberg, "High-brigthness output from a laser-diode array coupled to a phase-conjugating mirror," *Opt. lett.* **18**, p. 211, 1993.
7. M. Løbel, P. M. Petersen, and P. M. Johansen, "Single-mode operation of a laser-diode array with frequency-selective phase-conjugate feedback," *Opt. Lett.* **23**, p. 825, 1998.
8. B. Y. Zel'dovich, V. I. Popovichev, V. V. Ragul'skii, and F. S. Faizullo, "Connection between the wave fronts of the reflected and exciting light in stimulation mandel'shtam-brillouin scattering," *Sov. Phys. JETP Lett.* **15**, p. 109, 1972.
9. A. Yariv and D. M. Pepper, "Amplified reflection, phase conjugation and oscillation in degenerate four-wave mixing," *Opt. lett.* **1**, p. 16, 1977.
10. A. Ashkin, G. D. Boyd, J. M. Dziedzic, R. G. Smith, A. A. Ballman, J. J. Levinstein, and K. Nassau, "Optically-induced refractive index inhomogeneities in $LiNbO_3$ and $LiTaO_3$," *Appl. Phys. Lett.* **9**, p. 72, 1966.
11. J. Feinberg, D. Heiman, A. R. Tanguay, and R. Hellwarth, "Photorefractive effects and light-induced charge migration in barium titanate," *J. Appl. Phys.* **51**, p. 1297, 1980.
12. D. R. Hall and P. E. Jackson, *The Physics and Technology of Laser Resonators*, IOP Publishing Ltd, 1989.
13. J. M. Verdiell and R. Frey, "A broad-area mode-coupling model for multiple-stripe semiconductor lasers," *IEEE J. Quan. Elec.* **26**, p. 270, 1990.
14. J. Feinberg, "Self-pumped, continous wave phase conjugator using internal reflections," *Opt. Lett.* **7**, p. 486, 1982.
15. Y. Fainman, E. Klancnik, and S. H. Lee, "Optimal coherent image amplification by two-wave coupling in photorefractive $BaTiO_3$," *Opt. Eng.* **25**, p. 228, 1986.
16. X. Tang, J. P. van der Ziel, and A. K. Chin, "Characterisation of the array modes of high-power gain-guided GaAs single-quantum-well laser arrays," *IEEE J. Quan. Elec.* **32**, p. 1417, 1996.
17. M. Løbel, *Improvement of the Coherence Characteristics of Laser Diode Arrays Using Photorefractive Phase Conjugation.* PhD thesis, Risø National Laboratory, 1998.